^{7}Li(p, n_0)^{7}Be angular distributions to E_p = 3.8 MeV*

C. A. Burke,† M. T. Lunnon, and H. W. Lefevre
Department of Physics, University of Oregon, Eugene, Oregon 97403
(Received 17 June 1974)

Differences between results from earlier measurements of the ^{7}Li(p, n_0)^{7}Be differential cross section have prevented use of the neutron spectrum from this reaction as a standard of neutron intensity. Differential excitation curves for the reaction were obtained at 17 angles for proton energies between 2.1 and 3.8 MeV. A pulsed proton beam incident upon a thick lithium metal target produced continuous neutron spectra which were measured by time of flight. The data were corrected for neutron scattering from the target. The neutron detector efficiency was determined through a simultaneous normalization of the measured angular distributions to the known total cross section at all proton energies. The efficiency determination was judged to be uncertain to about 5%. Resultant differential excitation curves have uncertainties between 5 and 8%. The zero degree differential cross section (E_p = 1.89 to 3.8 MeV), and the excitation functions and Legendre coefficients (E_p = 2.09 to 3.80 MeV), are presented in 10-keV increments and compared with other measurements.

[NUCLEAR REACTIONS ^{7}Li(p,n_0), E = threshold to 3.8 MeV; time of flight, plastic scintillator, deduced efficiency; measured $\sigma(\theta)$. Natural target.]

I. INTRODUCTION

The ^{7}Li(p,n)^{7}Be reaction is widely used as a neutron source in the keV to MeV neutron energy range. Prominent features of the reaction include a sharp reaction threshold at a proton energy E_p = 1.881 MeV, a peak a few hundred keV wide in both the total cross section and zero degree neutron yield near E_p = 2.25 MeV, and angular distributions peaked in the forward direction. There is a large kinematic variation of neutron energy with angle for a given proton energy.

Measurements of the ^{7}Li(p,n)^{7}Be reaction cross sections span more than 20 years. Table I summarizes the measurements,[1-10] including cross section type and detection method. The 1958 and 1959 total cross section measurements of Ref. 3 have been used for the normalization of the later angular distribution measurements. It is disappointing that different measurements show differences of up to 20% in the P_1 coefficient in Legendre expansions of the angular distributions.[8]

The primary problem in the measurements is that of knowing the efficiency of the neutron detector, which is defined at any neutron energy as the ratio of the number of neutrons detected to the number incident upon the detector. Efficiencies may be either calculated or measured. For conventional recoil scintillation detectors, calculations of efficiency at the required accuracy are not feasible if the incident neutron energy is much larger than the detector bias level because of poorly known contributions from secondary effects in the scintillator. In these cases, efficiencies are better measured, using a standard of neutron intensity. If the yield as a function of energy was well known, the zero degree neutron spectrum from protons bombarding a thick lithium metal target would make an ideal absolute neutron intensity standard. This spectrum has already been used at this laboratory to guide a calculation of detector efficiency,[11] and to define the low-energy neutron detection efficiency for our detector.[12]

However, when that efficiency is applied to measurements of the ^{12}C(d,n_0)^{13}N angular distributions, disagreements with published total cross sections emerge.[12] This suggests that errors in the ^{7}Li(p,n)^{7}Be zero degree yield might be responsible.

For the above reasons, further study of the ^{7}Li(p,n)^{7}Be reaction was deemed desirable. We report here measurements of ^{7}Li(p,n_0)^{7}Be angular distributions for proton energies up to 3.8 MeV and emission angles through 160°.

II. EXPERIMENTAL DETAILS

The University of Oregon Van de Graaff accelerator delivered a pulsed proton beam onto a lithium target centered in a neutron shield. Details of the 1 nsec full-width-at-half-maximum pulsed beam production have been reported elsewhere.[13,14] The spectrometer geometry is shown in Fig. 1. The source shield included two cylindrical tanks, one above and one below a movable central layer. Each tank was filled with a lithium carbonate-water slurry to moderate and absorb neutrons with minimum γ-ray production. The source shield reduced time-dependent background in the time-of-flight

TABLE I. Summary of experimental work on the $^7Li(p,n)^7Be$ reaction.

Measured quantity (accuracy)[a]	Method[b]	Proton energy range[c] (MeV)	Ref. No.	Year
$\sigma_T, \sigma(\theta)$	(m)	$E_{th}-2.5$	1	1948
σ_T	(l)	$E_{th}-2.5$	2	1957
σ_T (5% absolute, 1% relative)	(p)	$E_{th}-5$	3	1958–9
$\sigma(\theta), \sigma(0°)$ (5%)	(l)	2.27, $E_{th}-3$	4	1959
$\sigma_T, \sigma(\theta)$ (8%)	(t)	2.6–4	5	1961
$\sigma_T, \sigma(\theta), \sigma(0°)$ (7%)	(t)	3–10	6	1963
$\sigma(\theta), \sigma(0°)$ (3.5%)	(l)	$E_{th}-3$	7	
$\sigma(\theta)$ (10%)	(t)	$E_{th}-2.36$	8	1967
$\sigma(\theta), \sigma(0°)$ (6%)	(g)	< 2.45	9	1970
$\sigma(\theta), \sigma(0°)$ (12%)	(t)	2.6–5.4, 2.2–5.4	10	1972

[a] σ_T, $\sigma(\theta)$, and $\sigma(0°)$ denote total cross section, angular distribution, and zero degree yield, respectively.

[b] Method of measurement: (m), manganese bath; (l), long counter; (p), 4π graphite moderated neutron detector; (t), time of flight; and (g), gas filled proportional counter measurement.

[c] $E_{th} = 1.881$ MeV, reaction threshold.

(TOF) spectra sufficiently to eliminate the need for recording background spectra. When the source shield was not used, time-dependent background spectra were evaluated by recording "shadowbar backgrounds." These open geometry background spectra were measured with a 40-cm long by 5-cm diam brass shadowbar placed midway between the target and the detector.

The low mass target assembly diagrammed in Fig. 2 was used to reduce the effects of neutron scattering. Lithium targets were prepared under hexanes to retard oxidation. 99.9% pure lithium metal ribbon (Matheson, Coleman, and Bell, Norwood, Cincinnati, Ohio) was surface cut with a taut wire to approximately 1-mm thickness. Next, the open-ended target holder was pressed onto a 1-cm diam disk of the freshly exposed lithium. The target holder with target disk attached was then lifted from the hexanes and immediately coupled to the target chamber. The hexanes inside the target holder were removed by a forepump before opening the target chamber to the main vacuum system, which was maintained at 5 μTorr. The target disk was kept sealed to the target holder by atmospheric pressure. The outside of the lithium target was then coated with a thin film of grease to slow oxidation and was cooled with a jet of air.

The neutron detector was mounted on a cart which allowed flight paths of up to 3 m and angular displacements of 160°. Neutrons were detected through proton and/or carbon recoils in a 6.3-cm diam×1.3-cm thick Naton 136 (Koch-Light Laboratories Ltd., Scintillator Division, Colnbrook, Buckinghamshire, England) plastic scintillator. The scintillator was optically coupled to an RCA

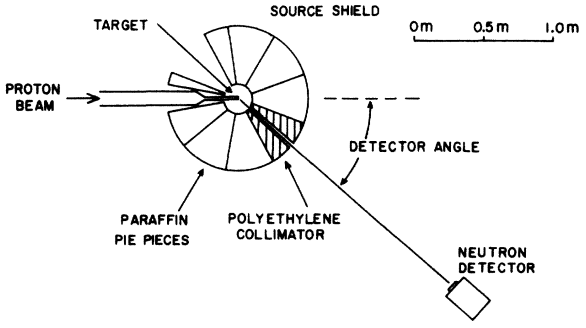

FIG. 1. Horizontal cross section of the experimental geometry. The source shield included cylindrical tanks above and below the central section shown. Paraffin sections opposite the collimator were removed to prevent backscattering from within the shield into the detector.

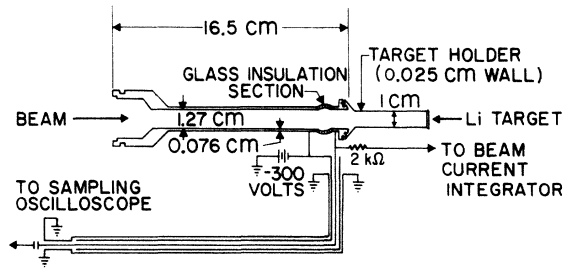

FIG. 2. Cross sectional view of the target chamber and lithium target assembly. The pulsed beam was monitored through the capacitive target pickoff, time-averaged (dc) target current was collected through the resistor. The target holder was 5 cm long, and sealed to the chamber via an "O" ring.

C70133B photomultiplier tube. Magnetic shielding of the detector decreased the position and angle dependence of phototube gain to below the 1% level. Temperature and counting rate changes caused at most 0.5% phototube gain changes. With our high gain detector, 1, 2, and 3 photoelectron events could be resolved in the pulse height spectra. Measurement of the ^{7}Li$(p,n_0)^7$Be angular distributions at proton energies near threshold required the detection of low energy neutrons and thus a low detector bias. The pulse height bias level was set at $\frac{1}{20}$ of that from the total absorption peak of 60-keV γ rays from ^{241}Am. For our detector this peak corresponded in pulse height to 39 photoelectrons from the photocathode. A low walk fast discriminator,[15] with threshold set below the linear bias level, provided time definition for each detected event.

Neutron TOF was converted to an analog signal by an Ortec time-to-amplitude converter (TAC). TAC signals were digitized by a Nuclear Data 161F analog-digital converter (ADC). The system was calibrated using the method described by Hatcher.[16] Data were corrected for ADC deadtime by using an Ortec current integrator and routing its output pulses through the ADC livetime clock. Digitized detector data and clock counts were accumulated in a DEC PDP-7 computer. At the conclusion of a TOF spectrum accumulation, the spectrum was written onto magnetic tape for later retrieval and analysis. Figure 3 shows a continuous neutron TOF spectrum measured at zero degrees with 3.4-MeV protons incident on the thick lithium metal target. The γ-ray peak is at the right. Ground state neutrons of maximum energy arrive at the detector at t_0. Neutrons to the first excited state of ^{7}Be appear as a step in the spectrum for $1/V > t_1$. The region between the prompt γ-ray peak and the ground state neutron kinematic edge gives a measure of the time-independent background.

In the past, experimentalists have not been able to measure the ^{7}Li$(p,n)^7$Be thick target spectrum because of high counting rates.[17] In this experiment, the effects of electronic and target-detector deadtime were reduced by spacing the beam pulses either 8 or 16 μsec apart to keep average target currents below 0.5 μA. Absence of deadtime effects at the 1% level was verified by accumulating data at different rates and comparing.

TOF spectra from ^{7}Li$(p,n)^7$Be were accumulated at angles 0 to 160° in 10° steps for each of four incident proton energies $E_p = 2.4$, 2.9, 3.4, and 3.9 MeV. Because of neutrons to the first excited state of ^{7}Be, neutron energies are a double valued function of proton energy over substantial ranges of energy and angle. In order to uniquely relate detected neutron energy to proton energy, only ground state neutron yields were used. Because of the reaction Q values, maximum energy ground state and first excited state neutrons are separated by about 500 keV. Within this window (defined by flight times t_1 and t_0 in Fig. 3) only ground state neutrons contribute to the spectra. Ground state neutron data from such windows were extracted from the data sets at each angle. As only four incident proton energies were used to measure the neutron yield at each angle there were regions of missing data in the composite spectra because the ground state data windows were separated. The missing ground state neutron data in the composite spectra were approximated by linear interpolation. The accuracy of the interpolation is discussed in Sec. IV.

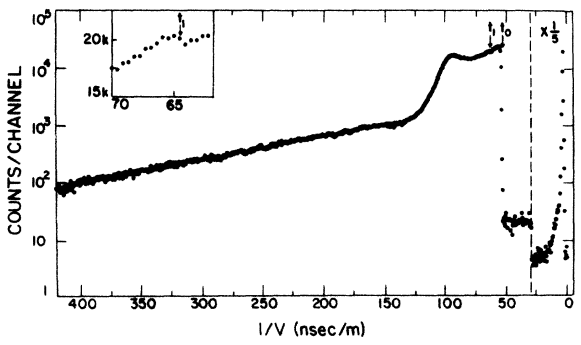

FIG. 3. A zero degree neutron time-of-flight spectrum resulting from 25 μC of 3.4-MeV protons bombarding a thick lithium metal target. The data were taken with a neutron flight path of 2.2 m and a channel width of 1.016 nsec.

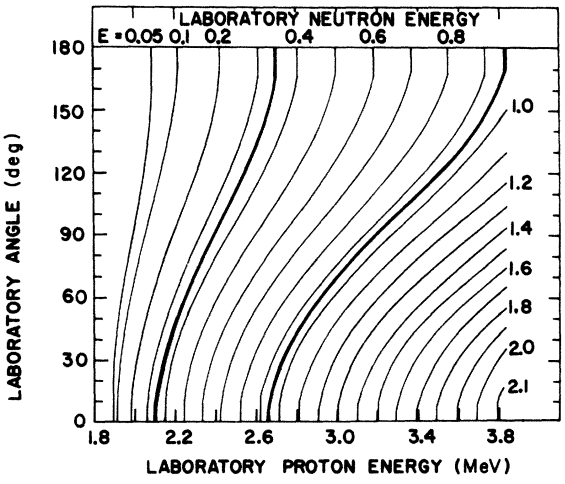

FIG. 4. Traces of constant laboratory neutron energy versus laboratory proton energy and reaction angle for ^{7}Li$(p,n_0)^7$Be. The wide lines delimit the neutron energies for which complete angular distributions were obtained.

III. DATA TRANSFORMATION AND NORMALIZATION

The kinematic relationship between neutron energy and proton energy can be seen in Fig. 4, where several lines of constant neutron energy are mapped as a function of proton energy and reaction angle. These lines of constant neutron energy are equivalently lines of constant neutron detection efficiency since, for a fixed detector bias, the efficiency is a function only of neutron energy. Before normalizing measured angular distributions to a total cross section, one must know the variation of detector efficiency with neutron energy. The detector efficiency determination, therefore, cannot result from a direct normalization at each proton energy of the measured angular distribution to the total cross section. We will show, however, that it is possible to simultaneously normalize the whole data set to the total cross section when the data set contains most proton energies. One is then able to deduce a correction to a first order detector efficiency.

The detected neutron yield at each angle θ_i can be expressed as a function of proton energy:

$$Y_i(E_p) = N_{ni}(\text{detected})\left(\frac{1}{n}\frac{dE_p}{dx}\right)\Big/(N_p dE_p d\Omega), \quad (1)$$

where $(1/n)(dE_p/dx)$ is the atomic stopping cross section, N_p is the total number of protons incident on the target, and $d\Omega$ is the solid angle subtended by the detector. N_{ni}(detected) is the number of counts in the TOF spectrum for proton energies between E_p and $E_p + dE_p$. The transformation channel width, dE_p, and E_p itself are determined from the neutron time of flight by the kinematic relationship between them at an observation angle θ_i. Such histogram transformations have been described by Wylie, Bahnsen, and Lefevre.[18] The proton energy yield is related to the differential cross section by

$$\sigma(\theta_i) = Y_i(E_p)/\epsilon(E_{ni}), \quad (2)$$

where $\epsilon(E_{ni})$ is the unknown efficiency of our detector for neutrons of energy E_{ni}. To first order, the neutron detection efficiency is simply the ratio of the zero degree neutron yield we observe in an experiment to a zero degree differential cross section from the literature, $\sigma'(0°)$:

$$\epsilon_0(E_{n0}) = Y_0(E_p)/\sigma'(0°). \quad (3)$$

We then write

$$\sigma(\theta_i) = Y_i(E_p) f(E_{ni})/\epsilon_0(E_{ni}), \quad (4)$$

where f is a correction to ϵ_0 which must now be deduced. For discrete measurements of the yield at l angles separated by equal increments $\Delta\theta$, the total cross section may be approximated by

$$\sigma_T = \sum_{i=1}^{l} 2\pi\sigma(\theta_i)\int_{\theta_i-\Delta\theta/2}^{\theta_i+\Delta\theta/2}\sin(\theta)d\theta$$

$$= 4\pi\sin(\Delta\theta/2)\sum_{i=1}^{l}\sigma(\theta_i)\sin(\theta_i). \quad (5)$$

If the efficiency correction is expressed as a power series in neutron energy,

$$f(E_{ni}) = \sum_{j=1}^{N} B_j E_{ni}^{j-1}, \quad (6)$$

the total cross section is obtained from (4) and (5) as

$$\sigma_T = 4\pi\sin(\Delta\theta/2)\sum_{i=1}^{l}\left[\frac{Y_i(E_p)\sin(\theta_i)}{\epsilon_0(E_{ni})}\left(\sum_{j=1}^{N} B_j E_{ni}^{j-1}\right)\right]. \quad (7)$$

Upon interchanging the order of summation, (7) becomes

$$\sigma_T = \sum_{j=1}^{N}\left[\sum_{i=1}^{l}\frac{4\pi\sin(\Delta\theta/2)Y_i(E_p)E_{ni}^{j-1}\sin(\theta_i)}{\epsilon_0(E_{ni})}\right]B_j. \quad (8)$$

The interior sum can be evaluated for each j since E_{ni} is kinematically related to E_p and θ_i. Denoting the interior sum A_{mj} for the mth proton energy, we may write

$$(\sigma_T)_m = \sum_{j=1}^{N} A_{mj}B_j. \quad (9)$$

The entire data set can thus be written in matrix notation as

$$\vec{\sigma}_T = \mathsf{A}\vec{B}, \quad (10)$$

where $\vec{B}$ is the column vector of unknown coefficients in the power series correction to ϵ_0, and A is a matrix whose elements are obtained from the measured yields, the reaction kinematics, and $\sigma'(0°)$. One can then use standard least squares techniques to obtain the $\vec{B}$ which will minimize the mean square deviation of σ_T calculated with (10) from the best measurements of σ_T.

Transformation and normalization of our data set to obtain A [Eq. (10)] required the atomic stopping cross section, a zero degree differential cross section and the total cross section for the ground state reaction. The atomic stopping cross section, corrected for the isotopic abundance of ^{7}Li atoms when used in Eq. (1), was calculated using the relativistic Bethe formula with shell corrections[19] with an ionization potential of 38.8 eV.[20] Calculated values of the stopping cross sections agree within 1% with those obtained by Janni[21] for

$E_p > 2$ MeV, and were within the 3% quoted accuracy of the experimental data of Bader *et al.*[22] for proton energies between 1 and 2 MeV. Nanosecond timing resolution and neutron flight paths of 3 m gave better than 10-keV neutron energy resolution. TOF data were therefore transformed to detected yield as a function of proton energy using a 10-keV proton energy interval. The zero degree excitation function of Eq. (3) was a composite which included the data of Bergström *et al.*[8] from threshold to $E_p = 2.2$ MeV and Austin's data[7] at higher energies.[23] ϵ_0 was tabulated in 10-keV steps and is shown in Fig. 5. The total cross section for neutron production given in Ref. 3 (Ref. 24) includes neutrons to the first excited state of ^{7}Be. The ground state total cross section was obtained from these results by subtracting the first excited state total cross section.[5] The ground state total cross section was assigned 5% uncertainties in the simultaneous normalization procedure. The normalization procedure included only the proton energies ($2.09 \leq E_p \leq 3.80$ MeV) for which we obtained complete angular distributions. The dark lines in Fig. 4 delimit the neutron energies for which there were complete angular distributions. Complete angular distributions were not obtained below 2.09 MeV because the energy of backangle neutrons was below the detector bias.

Correction functions [Eq. (6)] with values of $N \leq 7$ were investigated in this work, as was a Fourier series in E_n rather than a power series. Final choice of the correction function was guided by the ^{7}Li(p,n) cross sections in the literature and the physics of the neutron detector. A third order power series in neutron energy was finally chosen for the correction function. That function gave both a good fit to the total cross section and a reasonable shape to the individual differential cross sections. The resultant efficiency ϵ is shown in Fig. 5. The increased efficiency of the neutron detector over the calculated recoil proton efficiency, which is also shown in Fig. 5, is due mainly to detection of carbon recoil scintillations. That carbon recoils account for about one-third of the neutron detector efficiency at 2 MeV for an Am/20 pulse height bias was shown in a separate experiment and has been reported elsewhere.[25] The zero degree neutron yield of our measurement and normalization is shown in Fig. 6(a).

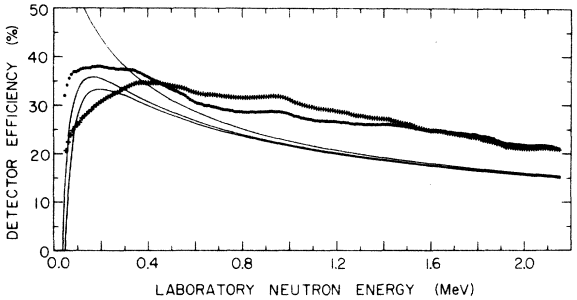

FIG. 5. The neutron detector efficiency, ϵ (dotted line) compared with the first order efficiency, ϵ_0 (cross-hatched line). Also shown is the result of a first order hydrogen recoil efficiency calculation, $\epsilon_H = (1 - e^{-n\sigma l}) \times (1 - B/E_n)$, where n is the number density of hydrogen atoms in the Naton scintillator, l is the thickness of the scintillator, and σ is the (n,p) cross section at the neutron energy E_n. The three lines correspond to biases, B, of 0, 40, and 50 keV.

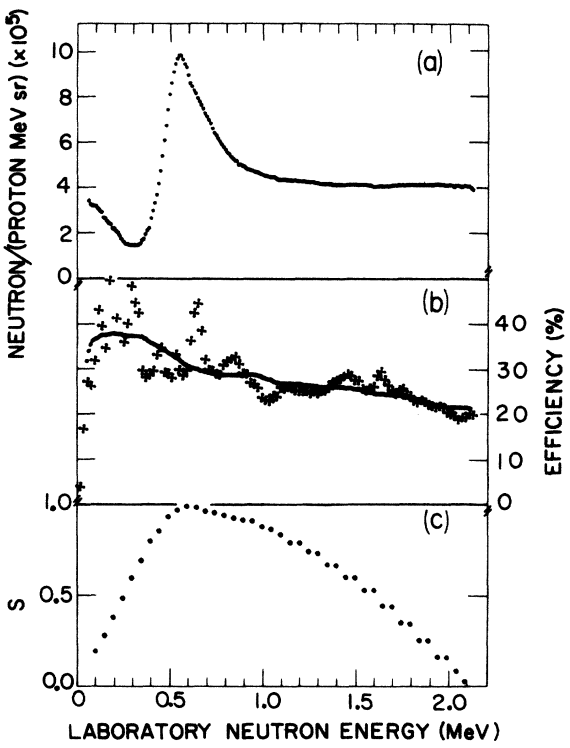

FIG. 6. (a) The natural Li(p,n_0) zero degree neutron energy yield of this work. (b) A comparison of the relaxation (pluses) and least squares (dots) solutions for the neutron detector efficiency. (c) The efficiency weight function vs neutron energy, normalized to a maximum value of unity.

IV. CORRECTIONS AND UNCERTAINTIES

As protons slow down and stop in a thick lithium metal target, nuclear reactions remove less than 0.01% of the incident protons. Small angle Coulomb scattering is calculated to give an rms scattering angle $<1.5°$ for all proton energies above the reaction threshold.[18]

Neutron spectra are affected by scattering from the target and from the neutron collimator. Target scattering and attenuation of neutrons was evalu-

ated at each angle by comparing spectra taken with a target and target holder of double the normal mass with spectra taken with the regular target. The data were separately corrected for the neutron scattering cross section of lithium which has a resonance at $E_n = 250$ keV. The corrections to the data resulted from extrapolation to zero target and target holder mass. The angle and energy dependent yield uncertainty due to all target scattering corrections was less than 3%. Inscattering from the collimator was found to vary both with the collimator details and with the neutron flight path but the inscattering correction was nearly independent of neutron energy. It was determined by open geometry measurements with shadow bar evaluation of background. The uncertainty in this 2 to 7% correction resulted in a 1% uncertainty in the yields. Air attenuation of the neutron flux was calculated to be a maximum of 2%, and this effect was ignored and is thus included in $\hat{B}$ [Eq. (10)].

The energy scale of the neutron spectrometer was tested using a lead filter and iron resonance lines. Neutron energy transformations of TOF spectra taken with a lead filter showed a transmission minimum within ±2 keV of the reported scattering resonance at 530-keV neutron energy.[26] Another check on the neutron energy scale was obtained from dips in the TOF spectra caused by iron resonances in the detector magnetic shield. The energy positions of these dips agreed to within 1% with the iron resonance neutron energies given in BNL-325.[27]

Uncertainty in charge integration, including the live time measurement system, was 0.1%. TOF spectra were accumulated for preset amounts of charge (typically 100 μC) chosen to give 1% counting statistics in the neutron TOF data. Data reproducibility was determined to be better than 3% by comparing neutron energy transforms of data taken under different experimental conditions over a six month span.

Proton energy ranges for which we used an interpolation to approximate the ground state data (see Sec. III) were 2.34–2.43, 2.78–2.98, and 3.28–3.49 MeV. Interpolations were assigned statistical uncertainties of 5% on the basis of a comparison of the interpolations with measured results for an excitation function at zero degrees.

Table II lists the uncertainties in the data sets and the energy ranges and angles to which they apply. As the uncertainties result from independent effects, they were compounded quadratically. The normalization procedure eliminated any uncertainty in the cross sections due to uncertainties in the proton stopping power. Those uncertainties only appear in the efficiency correction function.

Two tests were made to see whether the least squares normalization of the angular distribution at all proton energies gave a believable detector efficiency. First, a relaxation technique was used instead to normalize the angular distribution. In that technique, an arbitrary starting detector efficiency is assumed (an efficiency which does not vary with neutron energy, for example). A total cross section is then calculated with that efficiency, at all proton energies, from the data. The starting efficiency is then changed by a small amount, one neutron energy at a time, in 20-keV steps. For each change at each energy the total cross section at all proton energies is recalculated to see whether an improved fit to the ORNL total cross section results. The process is then repeated until the results converge to a set of stable values. Several markedly different starting efficiencies were tested and they all converged pointwise to identical values. The resulting fit to the total

TABLE II. Uncertainties (%) in the data of this experiment, identified by source of uncertainty and data range so affected. Uncertainties for the interpolated regions are underlined.

Source	Forward angles	Back angles
Current integration	0.1	0.1
Counting statistics	1, 5	1, 5
Corrections:		
Collimator-flight path	1	1
Source scattering	1	3
Lithium resonance scattering $E_p \simeq 250$ keV ($E_p = 1.98$–2.06 MeV at 0°) (to 2.4–2.6 MeV at 160°)	2	2
Combined experimental uncertainties:		
At $E_n \simeq 250$ keV only	2.6, 5.6	3.9, 6.3
In general	1.7, 5.2	3.3, 5.9

cross section was within 0.1% everywhere, but the resulting efficiency variation with neutron energy was physically unreasonable. The relaxation forced an enhanced efficiency at $E_n = 640$ keV [Fig. 6(b)] which would cause unreasonable structure in the differential cross sections. When a third order power series in neutron energy is fitted to the relaxation solution for detector efficiency, however, it agrees within 2% at all neutron energies with the correction function f of Sec. III.

The second test of the detector efficiency was made by applying it to the yield of first excited state neutrons. That experimental yield was obtained from the total yield by subtracting the ground state yield deduced in this measurement. The ^{7}Li$(p,n_1)^7$Be differential cross sections which were thus obtained agreed within statistics with those from other measurements.[5,6]

To assign an uncertainty to the efficiency function ϵ, we first consider the efficiency determination process. In the normalization of the angular distributions to the total cross section, the fractional weight of any data point at a proton energy E_p and observation angle θ is, from Eq. (7),

$$s_{mi} = Y_i(E_{pm})\sin(\theta_i)\left(\sum_{j=1}^{N} \frac{B_j E_{ni}^{j-1}}{[\epsilon_0(E_{ni})\sigma_T(E_{pm})]}\right), \quad (11)$$

where m and i index proton energy and angle, respectively. The weight of neutrons of energy E_n on the efficiency determination is the sum of the fractional weights over all angles included in the normalization procedure at the proton energies associated with E_n,

$$s(E_n) = \left[\sum_i s_{mi}\right]_{E_n}. \quad (12)$$

This sum is along lines of constant neutron energy

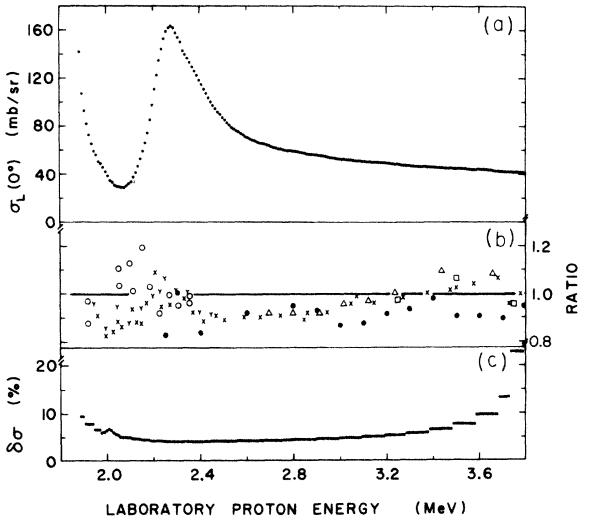

FIG. 7. The ^{7}Li$(p,n_0)^7$Be zero degree differential cross section (a) as determined in this experiment; (b) in ratio as others' results compared to ours: × Austin (Ref. 7), ○ Bergström *et al.* (Ref. 8), △ Bevington *et al.* (Ref. 5), □ Borchers and Poppe (Ref. 6), Y Peetermans (Ref. 9), ● Elbakr *et al.* (Ref. 10); (c) percentage uncertainties in our measurement.

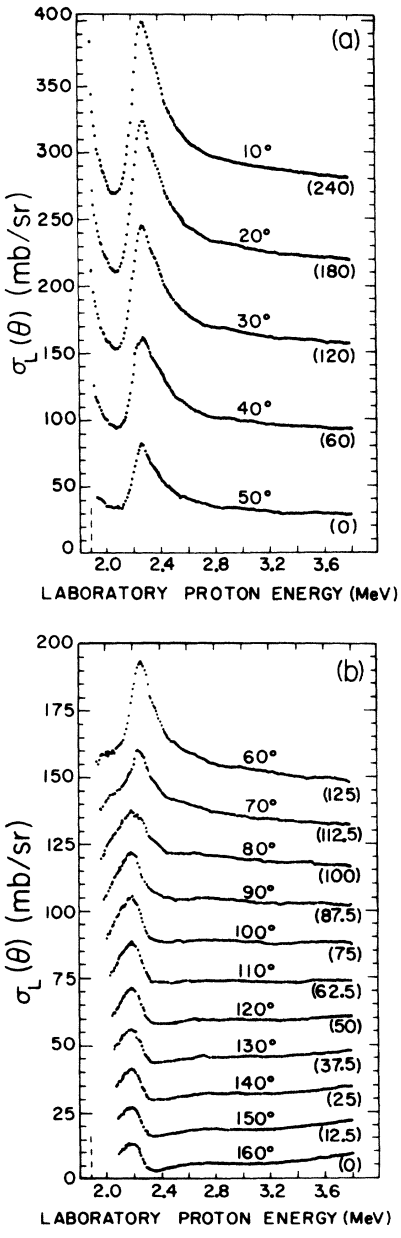

FIG. 8. ^{7}Li$(p,n_0)^7$Be excitation curves in 10° steps. Each curve is labeled by the reaction angle and a vertical offset in parentheses to be subtracted from the ordinate to obtain the cross section at that angle. Reaction threshold is marked as a vertical dashed line at 1.881 MeV. (a) Angles 10 through 50°; (b) angles 60 through 160°.

such as those shown in Fig. 4. We recall that only proton energies $2.09 \leq E_p \leq 3.8$ MeV are included, so that neutron energies outside the region bounded by the wide lines of Fig. 4 have progressively smaller fractional weights.

The weight versus neutron energy function defined by Eq. (12) was calculated, and the normalized result is plotted in Fig. 6(c). Note that the efficiency errors at intermediate neutron energies most sensitively affect the least squares fit to the total cross section. We postulate that the relative uncertainty in the efficiency is inversely proportional to the square root of the weight function s since s is proportional to the sum of the contributions to the efficiency determination at each E_n. From comparison of our integrated angular distributions with the total cross section, we conclude that there is a 4% minimum uncertainty in the differential cross sections due to the normalization. The estimate of the uncertainty in the efficiency itself must also include the 3% uncertainty in the stopping cross section, but that uncertainty did not affect the differential cross sections because of the normalization procedure. Thus the neutron detector efficiency is estimated to be known at best to 5%, and its uncertainty is inversely proportional to the square root of s plotted in Fig. 6(c).

V. RESULTS

Figure 7 presents the $^7\mathrm{Li}(p, n_0)^7\mathrm{Be}$ zero degree excitation function from this work and a comparison through ratio with other reported measurements. The uncertainty in our measurement shown in Fig. 7(c) was obtained by quadratically combining the data uncertainties with the uncertainty in the detector efficiency (exclusive of uncertainties in the stopping power). Our results for the zero degree excitation function lie between those of Bergström *et al.*[8] and those of Austin[7] at the lowest energies; agree with those of Bergström *et al.*[8] and Peetermans[9,28] between 2.2 and 2.4 MeV; are about 10% higher than other measurements between 2.4 and 2.9 MeV; and agree within uncertainties at higher energies. The disagreement for $2.4 < E_p < 2.9$ MeV is outside the combined uncertainties of the measurements. However, this proton energy range includes ground state neutrons with $0.7 < E_n < 1.2$ MeV, and our neutron detector efficiency is better defined by the normalization procedure at these energies than elsewhere.

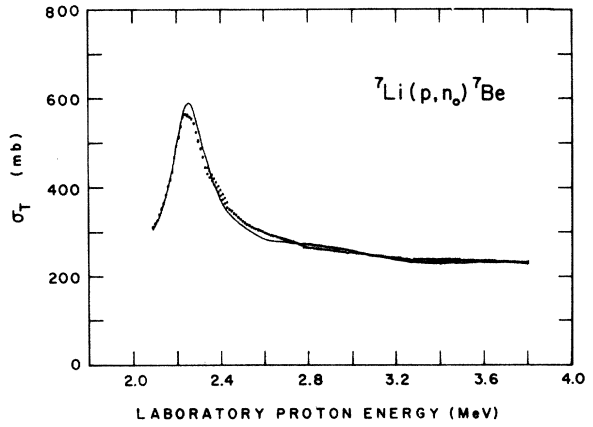

FIG. 9. Lengendre coefficient $a_0 \pm \delta a_0$ of this work (dots) compared with the ground state total cross section (Refs. 3 and 5) (line). δa_0 is the uncertainty resulting from uncertainties in the differential cross sections.

Differential excitation curves at each angle are shown in Fig. 8. A Legendre polynomial expansion, through order six, of the differential cross section in the center of mass system was made at each proton energy, as

$$4\pi\sigma(\theta_{\mathrm{c.m.}}) = \sum_{i=0}^{6} a_i P_i(\cos\theta_{\mathrm{c.m.}}) . \tag{13}$$

We found that the first three terms of the expansion were adequate to reproduce the differential cross section within 5% for angles less than 130° and within 10% for larger angles. The zero degree cross section from this work, and the Legendre coefficients and uncertainties, are tabulated in Ref. 29.

The coefficient of P_0 in the Legendre polynomial expansion is the total cross section. Figure 9 compares a_0 with the ground state total cross section from other measurements.[3,5] Maximum discrepancy between a_0 and the total cross section is 5% near $E_p = 2.3$ MeV. Elsewhere the agreement

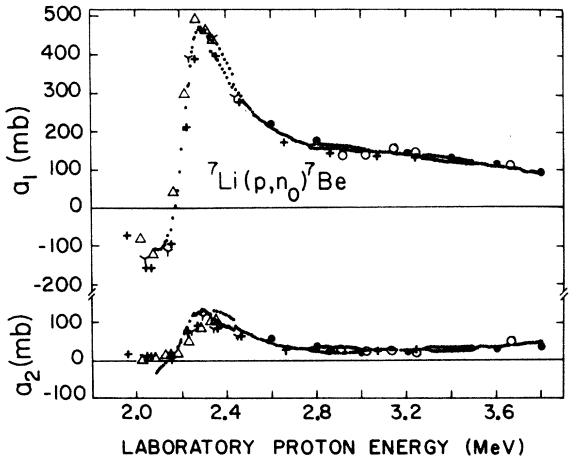

FIG. 10. The Legendre coefficients a_1 and a_2 for $^7\mathrm{Li}(p, n_0)^7\mathrm{Be}$. The results of this experiment (dots) are plotted as $a_i \pm \delta a_i$. The data are compared with those of Ref. 7 (+), Ref. 8(Δ), Ref. 5(○), Ref. 9 (Y), and Ref. 10 (●).

is better than 4%.

Legendre coefficients a_1 and a_2 are compared with previous experimental results in Fig. 10. We note that our a_1 is closest to those of Bergström *et al.*[8] and Peetermans[9] for $E_p < 2.4$ MeV. Our a_1 is 10% higher than Austin's[7] for $E_p > 2.2$ MeV, and is in agreement with that of Bevington *et al.*[5] for $E_p > 3$ MeV. a_2 of this work peaks at 2.3 MeV as do those of Austin[7] and Peetermans,[9] but lower than the a_2 peak reported by Bergström *et al.*[8] Also, a_2 is about 25% higher than other results at 2.2 MeV but agrees for $E_p > 2.8$ MeV. Ours is the only measurement to indicate negative values of a_2 at low energies.

Brown *et al.*[30] recently investigated the structure of the ^{8}Be nucleus through phase shift analyses of ^{7}Li(p,p) data and the (p,α), (p,p'), and (p,n) total cross section data for proton energies below 2.5 MeV. They found a previously unknown 3^+ level at 2.05 MeV as well as the 3^+ level at 2.25 MeV first assigned by Adair.[31] This perhaps explains the lack of success of the single-level resonance theory calculations which have been used in the past in attempts to fit the low energy Li(p,n) cross sections. A single-level resonance theory calculation brought to our attention the important point that a_0 and a_2 peak at different proton energies but we have not attempted a multilevel analysis. The experimental results presented herein hopefully will aid in future theoretical analyses.

VI. CONCLUSION

We intercompare the Legendre coefficients of our measurements with those from other measurements, and use the comparisons as an aid in deciding which zero degree yield is most nearly correct. First, none of the other measurements show a negative a_2 and there is not yet any theoretical reason to expect one. This suggests that one should weight the zero degree yield of this work less than that of others for $E_p < 2.2$ MeV. However, as shown in Fig. 7, our 0° results are nearly the average of those of Refs. 8 and 9 in this energy region. Secondly, that a_1 and a_2 of Austin's work[7] differ from those of this work, and those of Refs. 8 and 9, suggests weighting Austin's data[7] less than that of the others around $E_p = 2.3$ MeV. For $E_p > 3$ MeV, Austin's results[7] agree with others. Thus, we conclude that the 0° yield shown in Fig. 7 best represents the ^{7}Li$(p,n_0)^7$Be reaction.

We find, however, that if the ^{12}C(d,n) angular distributions of Ref. 12 were processed with an efficiency determined from the ^{7}Li$(p,n_0)^7$Be zero degree neutron yield of this work, that data would still disagree with the ORNL ^{12}C$(d,n)^{13}$N total cross section[32] by 18% at 1.2-MeV deuteron energy but would come into agreement at energies near 2 MeV. Errors in the ^{7}Li$(p,n_0)^7$Be zero degree yield are not responsible for the ^{12}C$(d,n)^{13}$N total cross section disagreement. At this point we can only say that the ORNL ^{12}C$(d,n)^{13}$N ground state total cross section cannot be consistently related at all energies to the ORNL ^{7}Li$(p,n)^7$Be total cross section through our differential cross sections for the two reactions. We are inclined to suspect that the ORNL 4π counter is more sensitive to differences in angular distribution that was indicated by the early tests.

We note that the ^{7}Li$(p,n_0)^7$Be differential cross sections are normalized to the ^{7}Li$(p,n)^7$Be total cross section of Ref. 3, and as such are dependent on any errors in the 4π counter results. With that caution, the ^{7}Li$(p,n_0)^7$Be zero degree yield has the characteristics required of a neutron intensity standard: it is large and is reproducible to 3%; it is known as a function of neutron energy to 5%. We thus point to the thick ^{7}Li$(p,n_0)^7$Be zero degree yield as a reproducible absolute intensity standard useful with a neutron TOF spectrometer and accurate charge integration.

ACKNOWLEDGMENTS

We are pleased to acknowledge helpful discussions with Professor J. C. Overley. We gratefully acknowledge the assistance of W. F. Schultz with the Van de Graaff facility and J. D. McDonald with the computer system.

---

*Work supported in part by the U.S. Atomic Energy Commission and by the National Science Foundation.

†Present address: Institute of Molecular Biology, University of Oregon, Eugene, Oregon 97403.

[1]R. Taschek and A. Hemmendinger, Phys. Rev. 74, 373 (1948).

[2]H. W. Newson, R. M. Williamson, K. W. Jones, J. H. Gibbons, and H. Marshak, Phys. Rev. 108, 1294 (1957).

[3]R. L. Macklin and J. H. Gibbons, Phys. Rev. 109, 105 (1958); J. H. Gibbons, and R. L. Macklin, Phys. Rev. 114, 571 (1959).

[4]F. Gabbard, R. H. Davis, and T. W. Bonner, Phys. Rev. 114, 201 (1959).

[5]P. R. Bevington, W. W. Rolland, and H. W. Lewis, Phys. Rev. 121, 871 (1961).

[6]R. R. Borchers and C. H. Poppe, Phys. Rev. 129, 2679 (1963).

[7]S. M. Austin, private communication [Austin's zero degree data are plotted in: H. W. Lefevre and G. U. Din, Aust. J. Phys. 22, 669 (1969)].

[8]A. Bergström, S. Schwarz, L. G. Strömberg, and

L. Wallin, Ark. Fys. 34, No. 14, 153 (1967).
[9]A. Peetermans, Ph.D. thesis, University of Liege, 1970 (unpublished).
[10]S. A. Elbakr, I. J. van Heerden, W. J. McDonald, and G. C. Neilson, Nucl. Instrum. Methods 105, 519 (1972).
[11]R. M. Bahnsen, W. R. Wylie, and H. W. Lefevre, Phys. Rev. C 2, 859 (1970).
[12]H. W. Lefevre, C. A. Burke, and R. M. Bahnsen, University of Oregon Report No. RLO-1925-44, 1971 (unpublished).
[13]W. R. Wylie, Ph.D. thesis, University of Oregon, 1969 (unpublished).
[14]University of Oregon, Nuclear Physics AEC Annual Progress Report, 1966.
[15]D. L. Wieber and H. W. Lefevre, I.E.E.E. Trans. Nucl. Sci. 13, No. 1, 406 (1966).
[16]C. Hatcher, E. G. & G. Nanonotes 1, 2 (1964).
[17]E. Barnard, A. T. G. Ferguson, W. R. McMurray, and I. J. van Heerden, Nucl. Instrum. Methods 34, 29 (1965).
[18]W. R. Wylie, R. M. Bahnsen, and H. W. Lefevre, Nucl. Instrum. Methods 79, 245 (1970).
[19]H. Bichsel, *American Institute of Physics Handbook* (McGraw-Hill, New York, 1963), 2nd ed., Chap. 8, p. 20.
[20]A. Dalgarno, Proc. Phys. Soc. (Lond.) 76, 422 (1960).
[21]J. F. Janni, Air Force Weapons Laboratory Technical Report No. AFWL-TR-65-150, 1966 (unpublished).
[22]M. Bader, R. Pixley, F. Mozer, and W. Whaling, Phys. Rev. 103, 32 (1956).
[23]In taking the ratio of measured to reported zero degree yields, it was necessary to shift Austin's data (Ref. 7) 5 keV toward lower energies to remove a sharp discontinuity in ϵ_0. In our experiment, proton energies were determined from the measured neutron TOF, reaction angle, and Q value using standard kinematic equations [J. B. Marion and F. C. Young, *Nuclear Reaction Analysis Graphs and Tables* (North-Holland, Amsterdam, 1968)]. This consistently put the $E = 2.25$ MeV peak in the zero degree yield 5 keV lower than other measurements [Ref. 7, and H. W. Lefevre and G. U. Din, Aust. J. Phys. 22, 669 (1969)]. Such differences between neutron energies determined directly by TOF measurements and those determined from the proton energy by kinematics have been noted before [R. B. Schwartz, R. A. Schrack, and H. T. Heaton, II, Bull. Am. Phys. Soc. 16, 495 (1971); National Bureau of Standards Monograph No. 138, January 1974 (unpublished); R. B. Schwartz, private communication].
[24]A redetermination of the efficiency of the 4π neutron detector by C. Johnson gave a result 2.2% lower than that used by Macklin and Gibbons (R. L. Macklin, private communication). All cross sections quoted in this paper have therefore been renormalized (multiplied by 1.022) if they were initially normalized to the total cross section as reported in Ref. 3.
[25]C. A. Burke and H. W. Lefevre, Nucl. Instrum. Methods 102, 357 (1972).
[26]R. B. Schwartz, R. A. Schrack, and H. T. Heaton, II, National Bureau of Standards Monograph No. 138, January 1974 (unpublished); R. B. Schwartz, private communication.
[27]*Neutron Cross Sections*, compiled by D. J. Hughes and R. B. Schwartz, Brookhaven National Laboratory Report No. BNL-325 (U. S. GPO, Washington, D. C., 1958), 2nd ed.
[28]We have normalized Peetermans's zero degree yield data (Ref. 9) to the zero degree data points from his measured angular distributions.
[29]C. A. Burke, Ph.D. thesis, University of Oregon, 1972 (unpublished).
[30]L. Brown, E. Steiner, L. G. Arnold, and R. G. Seyler, Nucl. Phys. A206, 353 (1973).
[31]R. K. Adair, Phys. Rev. 96, 709 (1954).
[32]R. J. Jaszczak, R. L. Macklin, and J. H. Gibbons, Phys. Rev. 181, 1428 (1969).